A EUROPEAN JOURNAL

CHEMPHYSCHEM

OF CHEMICAL PHYSICS AND PHYSICAL CHEMISTRY

REPRINT

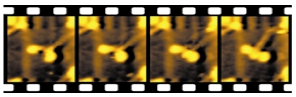

Molecular movements movie. The nanometer-scale dynamic movement of individual myosin V molecules (see picture) was captured in real time by a high-speed atomic force microscope (AFM). The AFM was designed to include a number of optimized components including feedback manipulation, high scanner bandwidths and stability, Q-control, and small cantilevers.

WILEY-VCH

CHEMPHYSCHEM

A High-speed Atomic Force Microscope for Studying Biological Macromolecules in Action

Toshio Ando,*[a] Noriyuki Kodera,[a] Yasuyuki Naito,[a] Tatsuya Kinoshita,[a] Ken'ya Furuta,[b] and Yoko Y. Toyoshima[b]

The atomic force microscope (AFM), which was invented by Binnig et al. in 1986, can image at nanometer resolution individual biological macromolecules on a substrate in solution. This unique capability awoke an expectation of imaging processes occurring in biological macromolecules at work. However, this expectation was not met, because the imaging rate with available AFMs was too low to capture biological processes. This expectation has at last been realized by the high-speed AFM developed by our research group at Kanazawa University. In this article, after a brief review of the development of our apparatus, its recent advancement and imaging data obtained with motor proteins are presented.

Introduction

A great variety of proteins perform very sophisticated functions not achievable with man-made creations. Hence, they are sometimes called biological "nanomachines." Motor proteins such as myosin, dynein, and kinesin are their representatives. The function of a protein is determined by its structure and is produced when the protein changes its structure dynamically. The nanometer-scale dynamic behavior of individual protein molecules cannot be captured by available techniques such as X-ray crystallography, NMR spectroscopy, and electron or optical microscopy. Therefore, we have to speculate upon the dynamic behavior of a certain protein from structural information given by these and other techniques. AFM[1] has made it possible for the first time to view the nanometer world in liquids.[4] This unique feature of AFM has been very welcome to the life sciences, because proteins can function solely in aqueous solution. Without any staining, it is possible to view living protein molecules at nanometer resolution. To image dynamic behavior of individual protein molecules with AFM, an additional feature, such as a high scan rate, must be implemented into the AFM. To do so, the various components involved in an AFM, such as cantilevers, scanners, and electronic devices, have to be optimized. If even one device cannot be optimized, the scan speed will be limited, resulting in a low scan rate. We have optimized every AFM component for high-speed scanning and succeeded in developing a high-speed AFM that can capture a 100×100-pixel image within 80 ms.[2, 3] In 2001, using the high-speed AFM to image myosin V molecules produced exciting movies, showing dramatic movement of the individual molecules weakly attached to a mica surface in solution.[2] This will be a turning point in the studies on biological nanomachines. High-speed AFM imaging of processes occurring in them may allow us to confirm directly what we have speculated about their dynamic behaviors, or may show what we have never imagined. Herein, first we briefly review the development of our high-speed AFM, and then we describe what we have been studying with the AFM since this development.

Results and Discussion

Rate-Limiting Factors

Here we summarize factors that limit the scan rate of AFM in the tapping mode of operation. The details are given in our previous papers.[2, 3] The rate-limiting factors are 1) the resonance frequency of cantilevers, 2) the root-mean-square (RMS)-DC conversion rate, and 3) the bandwidth of the z scanner. It is not very difficult to achieve the required bandwidths of the other electronic devices (see Figure 1). The time (T) required for getting one image consisting of $N \times N$ pixels is expressed by Equations (1) and (2):

$$T > 2nN^2/F_c \quad (1)$$

$$T = 2pN^2/V_s > 2pN^2/\lambda F_b \quad (2)$$

where n is the minimum number of waves of the input sinusoidal signals required for the accurate RMS-DC conversion, F_c the resonance frequency of a cantilever, p the pixel size, V_s the scan speed of the sample stage in the fast scanning direction

[a] *Prof. Dr. T. Ando, N. Kodera, Y. Naito, T. Kinoshita*
Department of Physics, Kanazawa University, Kakuma-machi
Kanazawa, Ishikawa 920-1192 (Japan)
Fax: (+81) 76-264-5739
E-mail: tando@kenroku.kanazawa-u.ac.jp

[b] *K. Furuta, Prof. Dr. Y. Y. Toyoshima*
Department of Life Sciences, Graduate School of Arts and Sciences
The University of Tokyo, Komaba 3-8-1, Meguro-ku
Tokyo 153-8902 (Japan)

  DOI: 10.1002/cphc.200300795

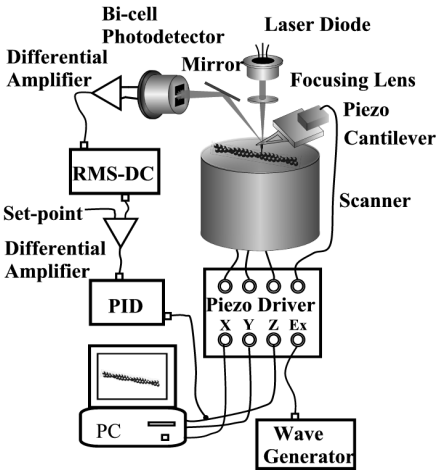

Figure 1. *A schematic of a conventional AFM system for the tapping mode of operation. The cantilever is oscillated by excitation with the electric piezo actuator. The laser beam reflected back from the cantilever is incident onto the bi-cell photodetector. The output from the differential amplifier represents the deflection of the cantilever. The output from the RMS-DC converter represents the oscillation amplitude of the cantilever. When the sample stage is scanned horizontally, the tip – sample interaction changes due to the variations of sample height, which resultsg in changes in the amplitude. The PID (proportional-integral-differential) feedback circuit detects the difference between this amplitude and its preset value, and outputs a signal to the piezo driver in order to move the sample stage vertically. This procedure is quickly repeated until the difference becomes zero. Thus, the cantilever's oscillation amplitude is kept constant during the scanning of the sample stage, and therefore, the movement of the sample stage follows the topography of the sample.*

(that is, the x direction), λ the apparent width of features on the surface, and F_b is the feedback bandwidth. The slowest device among those involved in the feedback loop is the z scanner. Therefore, F_b is approximately equal to the bandwidth of the z scanner. In order to develop a high-speed AFM, we first need cantilevers that have a high resonance frequency in water and a small spring constant. The dimensions of such cantilevers have to be very small.[2, 5] Therefore, the optical system for detecting the cantilever deflection has to be compatible with such small cantilevers.[2, 6] Next, we need an RMS-DC converter that can output the amplitude voltage of the input (slightly deformed) sinusoidal signals within one period of oscillation.[2] Otherwise, a higher cantilever resonance frequency is required. The scanner also has to move very quickly without unwanted vibrations.

Key Devices

Here, we briefly describe only the cantilevers and the scanner that we have developed, including recent improvements. For the other components, see our previous papers.[2, 3]

Cantilevers

As shown in Figure 2, we fabricated small cantilevers from silicon nitride using micromachining techniques. They are about 140 nm thick, 2 μm wide, and 9 μm long. The rear side of each cantilever is coated with 20 nm of gold. All surfaces of the cantilevers are further coated with 2 nm of osmium. The tip was

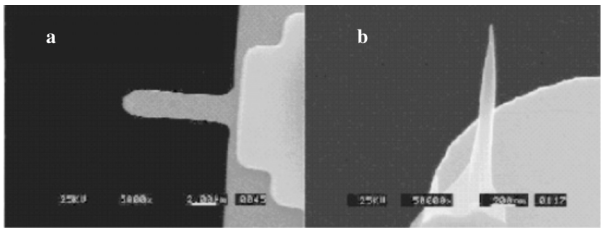

Figure 2. *Electron micrographs of the small cantilever developed for our high-speed AFM. a) The cantilever made from silicon nitride has no tip. b) A tip was grown on the cantilever free end by electron-beam deposition.*

grown by electron-beam deposition (EBD).[7] The tip length was adjusted to about 1 μm. Although the radius of the tip end ranges from 5 to 10 nm, the typical case is about 8 nm. The mechanical properties of the cantilevers were tested by measuring the spectra of their thermal motion. The resonance frequencies are about 1.5 MHz in air, and about 600 kHz in water, and the spring constants are estimated to be about 200 pN nm^{-1}. The resonance frequency in water can reduce the imaging time to 33 ms for 100×100 pixels [see Eq. (1)]. Recently, we found that the radius of the tip end can be made as small as 4 nm using a plasma etcher with argon gas. This technique is much simpler than attaching a carbon nanotube to the cantilever end.[8] The EBD tip is solid enough to scan samples many times without being damaged.

Scanner

After making and testing scanners with different designs, we reached the scanner shown in Figure 2 of ref. [2] and in Figure 6 of ref. [3] This scanner has a two-layered structure, with one layer for scanning in the y direction, and the second layer for scanning in the $\times$ and z directions. This layered structure allows small (but not zero) interferences between movements in the three axes. A sample stage is placed on the top of the z piezo actuator. The base to move in the x direction is tightly clamped in the z direction through steel ball bearings (Figure 3). This design allows this base to move smoothly in the x direction and suppresses vibrations in the z direction, even though this structure has a low resonance frequency in the z direction. In addition, the impulsive forces produced by the quick movement

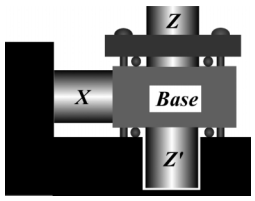

Figure 3. *Key mechanics for the scanner. The piezo actuators are 5 mm long, 4 mm wide, and 2.7 mm thick. The base ($6 \times 6.7 \times 2.7$ mm^3) is clamped in the z direction between two plates via six steel ball bearings (three for the top, and the other three for the bottom). The bearings are 1 mm in diameter. Each clamp is made using three screws placed close to each of the ball bearings. A sample stage is attached to the top of the z piezo. The impulsive force produced by quick movement of the z piezo is counteracted by the simultaneous displacement of the z′ piezo, in the opposite direction.*

of the *z* actuator are counteracted with the simultaneous displacements of the additional *z* actuator placed on the opposite side. This counterbalance is essential to reduce vibrations in the *z* direction further. The bandwidth of the *z* scanner reached about 60 kHz. Above 60 kHz, the resonant vibrations of the *z* actuators, around 100 kHz, lowered the performance of the *z* scanner. The fast scanning of the *x* scanner produced small vibrations in the *z* direction. The overall performance of our high-speed AFM is limited by the *x* and *z* scanners. Therefore, we still seek scanners with different designs for better performance. A classical design with blade springs is one possibility, although their dimensions should be small, and the counterbalance as above is absolutely indispensable. Another possibility for increasing the mechanical resonance frequency is to hold a piezo actuator at the center with a solid support, or at the both ends with blade springs, although the available displacement of the piezo actuator would be halved.

Imaging and Further Difficulties to Overcome

According to Equations (1) and (2), the feedback bandwidth of 60 kHz as well as the high resonance frequency of the small cantilevers can reduce the time for capturing an image with 100^2 2 nm pixels to 70 ms, as long as the apparent width of the sample is not too small. We investigated whether imaging can be carried out at (or near) the maximum rate predicted here. Myosin V (see Figure 4) directly attached to mica in solution was imaged successively (240 nm scan range; 100^2 pixels) for 1.6 s (20 frames). Myosin V, with a typical Y shape of the two head-neck regions and a long tail, was imaged. Only one head-neck region was attached to the mica surface; therefore, the other head and the tail were viewed to be moving rapidly (Figure 5).

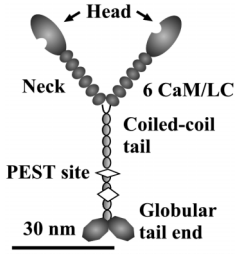

Figure 4. *Diagrammatic representation of chick brain myosin V. The head domain contains the ATP- and actin-binding sites. Calmodulin and light chains are associated with the six IQ motifs in the neck domain. The coiled coil regions in the tail are predicted from the amino acid sequence. In vivo, the globular tail ends bind a cargo to be carried by myosin V.*

Reduction of the Interaction Force

After this first success of real-time imaging of moving protein molecules, we tried to capture motor proteins moving along their tracks in the presence of ATP. Surprisingly, microtubules and actin filaments were progressively being broken during the successive imaging (Figure 6). This destruction seems to be caused by the tapping force exerted on the samples by the oscillating cantilever tip (we discuss this point later). There are several ways to reduce the tapping force: 1) Reduce the oscillation amplitude of cantilevers, 2) use Q-control[9] to optimize the cantilever oscillation, 3) reduce the spring constant of the cantilevers, and 4) adjust the set-point (that is, the cantilever oscillation amplitude to be kept constant during scanning) very close to the free oscillation amplitude (no tip–sample interaction). When imaging (Figure 6), the free oscillation amplitude of the cantilever is about 5 nm, and the set-point is 4.5 nm. This free oscillation amplitude is already close to the lower limit that can give acceptable images. Therefore, the first possibility (1) is removed from consideration. The oscillation of a cantilever with a high quality factor ($Q \approx$ a few hundreds) has a higher sensitivity to the tip–sample interaction compared with that with its natural Q value ($\approx 2-3$).[10, 11] However, this improvement is not compatible with the high-speed scanning because, in general, the oscillation amplitude of every oscillating system (not only cantilevers) with a high Q value cannot respond quickly to external influences. Actually, we have confirmed this general rule using Q-controlled cantilevers (Figure 7). Thus, possibility 2) is removed from consideration also. It may be

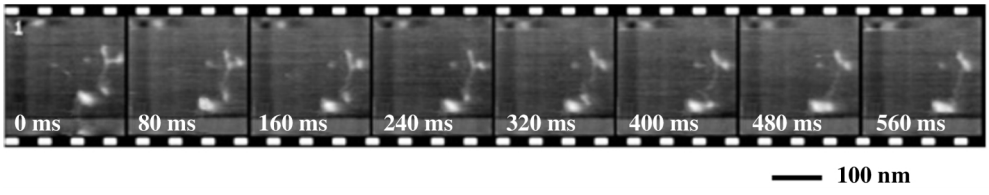

Figure 6. *Progressive destruction of a microtubule during imaging at 640 ms intervals. The microtubule is attached directly onto a mica surface. The same area of 400 × 400 nm² was imaged successively 15 times with 200 × 200 pixels. The tapping frequency is 590 kHz, the free oscillation peak-to-peak amplitude of the cantilever is 5 nm, and the set-point is adjusted at 4.5 nm. The six images are chosen from the successive 15 images. The number on each image indicates the frame number. The progressive destruction seems accelerated after the initial destruction.*

Figure 5. *Successive images, at 80 ms intervals, of myosin V on mica in buffer solution. The same area of 240 × 240 nm² was imaged 20 times with 100 × 100 pixels. Only the first eight successive images are shown. The tip speed is 0.6 mm s⁻¹ (scan rate, 1.25 kHz), and the frame rate is 12.5 s⁻¹. The tapping frequency is 600 kHz, and the free oscillation peak-to-peak amplitude of the cantilever is 5 nm. The reconstructed movie and the other movies can be viewed at the web site (http://www.s.kanazawa-u.ac.jp/phys/biophys/bmv_movie.htm).*

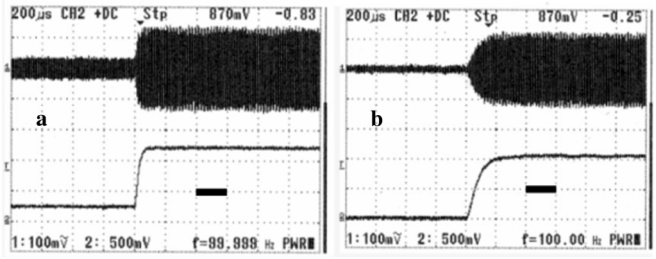

Figure 7. *Q-control effect on the response of a cantilever to the quick shift of the excitation frequency. The Q control circuit is home-made. The Q value of the cantilever with Q control was about 120, while its natural Q was about 3. The peak resonance frequency was 600 kHz. The excitation frequency was changed from 550 kHz to 600 kHz within a few ns a) without Q control, b) with Q-control. The upper traces show the time courses of the sensor output, and the lower traces show the time courses of the RMS-DC output. The scale bars indicate 200 μs. The response time of the Q-controlled cantilever is estimated to be about 80 μs, which approximately agrees with the theoretically expected value ($Q/\pi F_c \approx 64\ \mu s$).*

possible to reduce the spring constant of small cantilevers while keeping the resonance frequency high enough, but it requires years to develop such levers. When the set-point of an oscillating cantilever is set very close to the free oscillation amplitude, the tip tends to detach completely from the sample/substrate surfaces when the tip is scanning down a steep surface feature. Once detached, the tip does not land for a while on the surfaces because of the insufficient feedback due to a small difference between the set-point and the free oscillation amplitude (that is, feedback saturation). When the tip is not in contact with the surface, topographic information is completely lost (Figure 8a). However, it occurred to us whether we might be able to "manipulate" the feedback action for our purpose. The idea is as follows: When the cantilever amplitude becomes larger than the set-point and nearly the same as the free oscillation amplitude (that is, the tip is almost detaching from the sample surface), a DC voltage is added to the amplitude signal. This addition produces a large feedback signal, which results in a quick return of the cantilever oscillation amplitude toward the set-point. Thus, the set-point can be adjusted very close to the free oscillation amplitude without causing complete detachment of the cantilever tip from the sample/substrate surfaces. A similar manipulation can be applied when the cantilever oscillation amplitude becomes smaller than the set-point and can keep the tip from tapping the sample too hard. Using this technique, microtubules were successfully imaged repeatedly without destruction (Figure 8b). Details of an electronic circuit that performs these manipulations and of their effects on imaging are given elsewhere.[12]

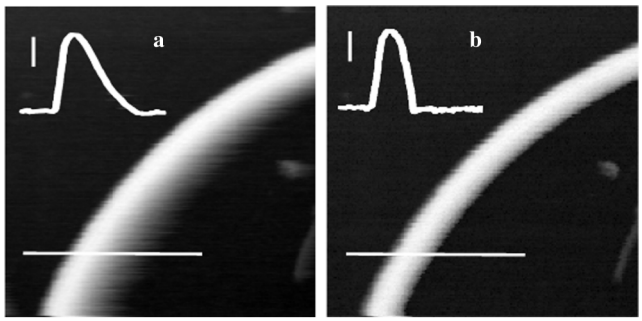

Figure 8. *The effect of the feedback manipulation on AFM imaging. The free oscillation peak-to-peak amplitude of the cantilever was 5 nm, and the set-point was 4.8 nm (very close to the free oscillation amplitude). These images with 200 × 200 pixels were obtained at 640 ms frame^{-1}. a) A microtubule imaged without the feedback manipulation. The cross section taken at the horizontal bar (200 nm) indicates that after passing the tops of the microtubule the oscillating cantilever tip completely detached from the sample/substrate surfaces. Vertical bar = 10 nm. b) A microtubule imaged with the feedback manipulation. The cross section taken at the horizontal bar (200 nm) shows a symmetric profile of the microtubule, which indicates that there was no complete detachment of the cantilever tip. The vertical bar, 10 nm. The repetitive imaging did not destroy the microtubule (data not shown).*

Imaging of Kinesin Moving along a Microtubule

After the implementation of this feedback-manipulation circuit to the AFM, kinesin molecules moving along microtubules were imaged. Compared with myosin V, kinesin is a very small motor protein. Therefore, we used a chimera protein (RK430G)—a homodimer composed of two heavy chains, which each consists of the head-neck region of kinesin at the *N*-terminal and gelsolin at the *C*-terminal. We found a kinesin molecule that was first moving randomly on mica, and then attached to a microtubule. After this attachment, the kinesin molecule moved along the microtubule. The velocity of the movement was about the same as expected from the ATP concentration used, which indicates that this movement is driven by ATP hydrolysis. Although the structural details of the kinesin molecule moving along a microtubule could not be resolved well, this observation clearly showed that repeated taps on a kinesin molecule with the oscillating cantilever tip did not inactivate the kinesin's motor and ATPase activities.

Imaging with Flash Photolysis of Caged Compounds

We have imaged myosin V molecules in the presence of ATP in order to examine whether or not a large structural change is produced at the head – neck regions during the ATPase reaction. Previously, we saw that the long tail of a myosin V molecule changed its orientation markedly in less than 30 ms.[2] However, we had to reserve judgment whether this large change was driven by ATP action, because we could not observe repeated orientational changes with the same myosin V molecule. The ATPase rate of myosin V alone is very small ($\approx 0.05\ s^{-1}$).[13] Therefore, to see its repetitive structural changes, we need to record images for a long time, which, in turn, requires the AFM to be stable for a long time without large drifts. Even when we can record stably for a long time, it is not easy to confirm if an observed structural change in a myosin V molecule is really driven by ATP action, because the world of small molecules in aqueous solution is quite noisy. In order to image the dynamic behavior of individual protein molecules, the molecules should not be firmly attached to a substrate surface. In such a condition, the protein molecules are always in Brownian motion. In addition, a structural change that is quite similar to the ATP-induced structural change may occur infrequently even in thermal equilibrium. A way around the difficulty is to image

protein molecules before and after changing the substrate concentration quickly. For this purpose, caged compounds[14] are quite useful because application of a UV flash for photolysis may not disturb the AFM imaging. We constructed a system for UV flash photolysis using a mercury lamp and a mechanical shutter. Since the high-speed AFM is mounted on an optical microscope, introduction of the UV flash system to the AFM was made simply by replacing the lamp house with the UV flash system, and by replacing the originally attached optical filters with appropriate UV filters. As a first try, myosin V was imaged using caged Ca^{2+}. Myosin V possesses six IQ motifs (consensus amino-acid sequences found in various calmodulin-binding proteins) at each extended neck domain to which a number of calmodulin molecules ($\approx 4-5$) and light chains ($\approx 1-2$) are attached in the absence of Ca^{2+}.[15] While in the presence of Ca^{2+}, some of these calmodulin molecules dissociate from myosin V.[16] Unexpectedly, the sample stage moved in the *x* direction during the application of a UV flash for 1 s, and soon returned after shutting off the UV light. This movement might be caused by thermal expansion of materials exposed to the UV light. During this period and even 3 s after shutting the UV light, nothing occurred in myosin V. However, after this, the following events took place (Figure 9): A head–neck in the left-hand side suddenly moved toward the right passing over the head–neck in the right-hand side, and simultaneously all calmodulin molecules (also the light chains) dissociated instantaneously from the neck regions, which resulted in very thin necks. In addition, the coiled-coil part, which had been connecting the neck–neck junction and the PEST (amino-acid motif that is thought to target cytoplasmic proteins for rapid proteolytic degradation) site, appeared to unwind. Next, myosin V was imaged using caged ATP. In this case, the sample stage did not move appreciably during UV light application. Before UV application, both the head–neck regions were roughly in the straight forms. After UV irradiation, one head–neck bent very quickly around the head–neck junction. The bending angle was almost 180°, so that the tip of the head became very close to the neck–tail junction. This bent conformation remained for about 2.5 s, and then it returned to the straight form. This bending/restretching behavior is very likely to be produced by ATP action. However, further studies remain to be done in order to confirm this causal relation and to identify the hinge region and the direction of bending in light of the 3D structural details of the head–neck domain. In addition, we have to know whether this bending or re-stretching takes place also in the actin-bound form in order to move the actin filament along its long filament axis.

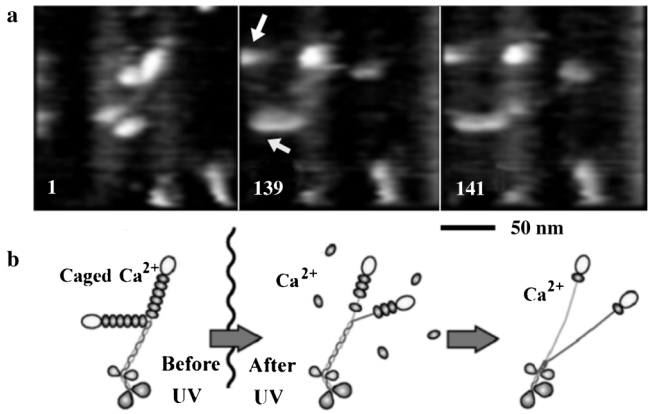

Figure 9. *Imaging with caged Ca^{2+}. a) Myosin V imaged before and after releasing Ca^{2+} from caged Ca^{2+} by UV flash photolysis. The same area of 200 × 200 nm² was successively imaged 300 times with 100 × 100 pixels at 80 ms intervals. The UV light was applied between the 81 st and 94th frames (for 1 s). At the 138th frame, the head–neck located on the left-hand side suddenly moved toward the right, and simultaneously both the neck domains became very thin. The number attached to each image indicates the frame number. The arrows indicate mirror images. The reconstructed movie is presented at http://www.s.kanazawa-u.ac.jp/phys/biophys/bmv_movie4.htm. b) Sketches of myosin V before and after UV light application.*

Future Improvements on High-Speed AFM

In the life sciences, it has long been a dream to view the nanometer-scale dynamic behavior of individual biopolymers in solution. The ability to acquire successive images every 80 ms will expand the scope of biological processes that can be examined in real time. However, there are biological processes that take place too fast for our high-speed AFM. What level of imaging rate can we reach? At present, the imaging rate of our AFM is limited by the scanner and by the small cantilevers. We have employed a triangle-wave form to drive the *x* scanner. The triangle wave form has high frequency components at the turning points. Therefore, when the *x* scanner changes its direction, unwanted vibrations tend to be produced. Moreover, due to the inertia of the mass, the turning cannot be done quickly, and mirror images are produced (see Figure 9). There may be two solutions to this problem. One is to afford a wider bandwidth to the mechanical structure of the *x* scanner and a lower mass by changing the material used. The other is to use a sinusoidal wave form to drive the *x* scanner and rescale the *x* coordinate of the image pixels. The latter is easier than the former, although in the latter the pixel density varies depending on the position in the *x* direction. In the *z* scanner, the bandwidth is determined almost exclusively by the resonance frequency of the piezo actuators used, as long as the counterbalancing method is employed. If a large displacement is not necessary in the *z* direction (ca. 500 nm at most), the bandwidth can be increased up to about 200 kHz. Thus, the imaging rate can be increased higher than video rate (ca. 40 frames s^{-1}).The resonance frequency of the small cantilevers that we have fabricated satisfies the condition for video rate already. In order to go far beyond 40 frames s^{-1}, the whole AFM architecture would have to be changed. At present, this seems far beyond our imagination.

Improvements to be made are not only for the temporal resolution, but also for the spatial resolution. The spatial resolution of AFM is determined by several factors: the radius of the cantilever tip end, electronic noise of the system, elastic deformation and movement of the sample caused by the tip–sample interaction, and movement of the sample caused by thermal agitations. The last factor appears only in high-speed imaging of dynamic behavior of biological macromolecules, because in such imaging the macromolecules should be tethered weakly to a substrate. Image blurring due to Brownian motion of the macromolecules has to be reduced only by

increasing the imaging rate. Movement of a sample due to the tip–sample interaction can be solved by reducing the interaction force.

We have devised a feedback manipulation method to reduce the interaction force. We first thought that the breakage of microtubules was caused by a large tapping force produced under our experimental condition. This inference motivated us to develop the feedback manipulation system. A recent study reported that when a force smaller than 500 pN is applied by a cantilever tip in the *z* direction onto microtubules on a substrate, microtubules are not collapsed.[17] We recently made a theoretical estimate of the tapping force under our experimental condition without the feedback manipulation, and found that it did not exceed 100 pN when averaged over the indention period. The feedback manipulation increases the feedback bandwidth and reduces not only the tapping force, but also the lateral force that is produced especially when an oscillating tip is crossing a steep up-hill topgraphic feature of a sample. Therefore, microtubules with height of 25 nm were likely to be destroyed by a large lateral force exerted from the cantilever tip oscillating with a peak-to-peak amplitude of 5 nm. Nevertheless, for better spatial resolution it is still important to reduce the tapping force by setting the free oscillation amplitude of a cantilever as small as possible, and by adjusting the set-point as close as possible to the free oscillation amplitude, by using the feedback manipulation technique. In order to make a further reduction of the tip-sample interaction force, we need to be able to detect the change in the cantilever oscillation more sensitively, without relying on Q control. The second derivative of the sensor's differential amplifier output may be more sensitive than the amplitude signal because the tip-sample interaction occurs much faster than the resonance frequency of the cantilever. To realize this, we need a sensor amplifier with a wider bandwidth and a stable and fast circuit to output the second derivative signal.

The capability that was expected of AFM, that is, imaging of biological processes in real time, has for the first time been realized by our high-speed AFM. Of course, as discussed above, much higher speed seems necessary for further expansion of the scope of biological processes that can be examined in real time. However, there are many biological samples that are waiting to be imaged even at 12.5 frame s^{-1}. For one year we have been trying to image motor proteins in action while finding and solving some difficulties. The AFM movies of individual motor molecules, such as kinesin moving along microtubules and myosin V bending its head–neck region after the ATP addition, clearly indicate the great value of viewing individual protein molecules at work at high resolution and in real time. We hope that high-speed AFM imaging will make a great contribution toward understanding the physics of biological nanomachines in the near future.

Experimental Section

Protein preparation: Myosin V was extracted from chick brains and purified as described.[13] Myosin V was stored at 0 °C in buffer A (25 mM KCl, 25 mM imidazole (pH 7.6), 2 mM $MgCl_2$, 1 mM EGTA (ethylene glycol tetraacetic acid), and 2 mM dithiothreitol). Tubulin was purified from porcine brain according to the method of Weingarten et al.[18] The purified tubulin was stored in liquid nitrogen until use. Microtubules were obtained by incubating the purified tubulin (≈2 mg mL^{-1}) at 37 °C for 20 min in the presence of 1 mM GTP (guanosine-5′-triphosphate), 5 mM $MgSO_4$, and 80 mM Pipes-KOH [1,4-piparazine-bis(2-ethanosulfonic acid) potassium hydroxide] (pH 6.8), and then stabilized with 40 μM taxol. To remove crumbs of the aggregated protein, hydrophobic beads (TSKgel Ether-Toyoperl 650, Tosoh, Japan) were added to adsorb them, and removed by centrifugation (16,000 g for 3 min). *N*-terminal 430 amino acids of rat kinesin fused to gelsolin (RK430G) was expressed in *E. coli* and purified using microtubule affinity as described.[19] The purified RK430G was frozen in liquid nitrogen and stored at −80 °C, and the thawed sample was used within 3 h.

AFM imaging: The AFM apparatus used was basically the same as used previously.[2] A drop (≈2 μL) of myosin V solution (≈7 nM) was placed on freshly cleaved mica (1 mm in diameter) for 3 min, rinsed with buffer A to remove unattached myosin V, and then imaged in buffer A without dithiothreitol. In the experiment with caged Ca^{2+}, myosin V was imaged in the presence of 20 μM caged Ca^{2+} (*O*-nitrophenyl EGTA (Molecular Probes, USA):$CaCl_2$ = 1:0.8) and 4 μM EGTA. In the experiment with cage ATP, 0.5 mM P^3-[1-(2-nitrophenyl)ethyl]-ATP (Dojindo Chemicals, Japan) was used. For imaging microtubules alone, a drop (≈2 μL) of microtubules (0.23 mg mL^{-1}) in buffer B (100 mM Pipes (pH 6.9), 1 mM $MgCl_2$, 1 mM EGTA, 20 μM taxol) was placed on a freshly cleaved mica surface for 3 min, rinsed with buffer B, and then imaged in buffer B (the concentration of taxol was reduced to 3 μM). For imaging kinesin and microtubules, the mica surface was first coated with anti-flag M2 monoclonal antibody (Sigma–Aldrich, 1 mg mL^{-1}; 2 μL, 3 min), and then washed with buffer B. Microtubules (0.23 mg mL^{-1}, 2 μL) were placed on the antibody-coated mica for 3 min, and rinsed with buffer B, and then imaged in a solution containing 3 μM kinesin, 5 μM ATP, and buffer B with 3 μM taxol.

Acknowledgements

This work was supported by the following grants to T.A.; the Proposal-based New Industry Creative Type Technology R&D Promotion Program from NEDO, Grants-in-Aid for Scientific Research from the Mitsubishi Foundation, the Naito Foundation and the Japan Society for the Promotion of Science (#14654071), and Special Coordination Funds for Promoting Science and Technology (Effective Promotion of Joint Research with Industry, Academia and Government) from the Ministry of Education, Sports, Science & Technology of Japan.

Keywords: kinesin · motor proteins · myosin V · real time imaging · scanning probe microscopy

[1] G. Binnig, C. F. Quate, C. Gerber, *Phys. Rev. Lett.* **1986**, *56*, 930–933.
[2] T. Ando, N. Kodera, E. Takai, D. Maruyama, K. Saito, A. Toda, *Proc. Natl. Acad. Sci. USA* **2001**, *98*, 12468–12472.
[3] T. Ando, N. Kodera, E. Takai, D. Maruyama, K. Saito, A. Toda, *Jpn. J. Appl. Phys.* **2002**, *41*, 4851–4856.
[4] O. Marti, B. Drake, P. K. Hansma, *Appl. Phys. Lett.* **1987**, *51*, 484–486.
[5] D. A. Walters, M. Viani, G. T. Paloczi, T. E. Shäffer, J. P. Cleveland, M. A. Wendman, G. Gurley, V. Elings, P. K. Hansma, *Proc. SPIE* **1997**, *3009*, 43–47.

[6] T. E. Shäffer, J. P. Cleveland, F. Ohnesorge, D. A. Walters, P. K. Hansma, *Appl. Phys. Lett*. **1995**, *80*, 3622 – 3627.
[7] D. J. Keller, C. Chih-Chung, *Surf. Sci*. **1992**, *268*, 333 – 339.
[8] Y. Nakayama, H. Nishijima, S. Akita, K. Hohmura, S. Yoshimura, K. Takeyasu, *J. Vac. Sci. & Tech*. **2000**, *B18*, 661 – 664.
[9] B. Anczykowski, J. P. Cleveland, D. Kruger, V. Elings, H. Fuchs, *Appl. Phys*. **1998**, *66*, 885 – 889.
[10] G. Haugstad, R. R. Jones, *Ultramicroscopy* **1999**, *76*, 77 – 86.
[11] S. Gao, L. Chi, S. Lenhert, B. Anczykowski, C. M. Niemeyer, M. Adler, F. Fuchs, *ChemPhysChem*. **2001**, *2001*, 384 – 388.
[12] a) N. Kodera, Y. Naito, T. Ito, T. Ando, *Biophys. J*. **2003**, *84*, 467a; b) unpublished results.
[13] T. Sakamoto, I. Amitani, E. Yokota, T. Ando, *Biochem. Biophys. Res. Commun*. **2000**, *272*, 586 – 590.
[14] S. R. Adams, R. Y. Tsien, *Ann. Rev. Physiol.* **1993**, *55*, 755 – 758.
[15] E. M. Espreafico, R. E. Cheney, M. Matteoli, A. A. C. Nascimento, P. V. De Camilli, R. E. Larson, M. S. Mooseker, *J. Cell. Biol*. **1992**, *119*, 1541 – 1557.
[16] A. A. C. Nascimento, R. E. Cheney, S. B. F. Tauhata, R. E. Larson, M. S. Mooseker, *J. Biol. Chem*. **1996**, *271*, 17 561 – 17 569.
[17] P. J. de Pablo, I. A. T. Schaap, C. F. Schmidt, *Nanotechnol*.**2003**, *14*, 143 – 146.
[18] M. D. Weingarten, A. H. Lockwood, S. Y. Hwo, M. W. Kirschner, *Proc. Natl. Acad. Sci. USA* **1975**, *72*, 1858 – 1862.
[19] J. Yajima, M. C. Alonso, R. A. Cross, Y. Y. Toyoshima, *Curr. Biol*. **2002**, *12*, 301 – 306.

Received: April 16, 2003 [F 795]

